PRAMANA
— journal of
physics

Vol. 65, No. 6
December 2005
pp. 1085–1096

Structural properties of low-density liquid alkali metals

A AKANDE[1], G A ADEBAYO[1,2] and O AKINLADE[2]
[1]The Abdus Salam International Centre for Theoretical Physics, Trieste, Italy
[2]Department of Physics, University of Agriculture, Abeokuta, Nigeria
E-mail: aakande@ictp.trieste.it; gadebayo@ictp.trieste.it; akinlade@yahoo.com

MS received 6 January 2005; revised 24 May 2005; accepted 22 July 2005

Abstract. The static structure factors of liquid alkali metals have been modelled at temperatures close to their melting points and a few higher temperatures using the reverse Monte Carlo (RMC) method. The positions of 5000 atoms in a box, with full periodicity, were altered until the experimental diffraction data of the structure factor agrees with the associated model structure factor within the errors. The model generated is then analysed.

The position of the first peak of the pair distribution function $g(r)$ does not show any significant temperature dependence and the mean bond lengths can be approximated within an interval of 3.6–5.3 Å, 4.5–6.6 Å, 4.8–6.7 Å and 5.1–7.3 Å for Na, K, Rb and Cs respectively. The cosine bond distributions show similar trend with the flattening up of the first peak with increase in temperature. In addition, the coordination numbers of these liquid metals are high due to the presence of non-covalent bonding between them. On the average, we surmise that the coordination number decreases with increase in temperature.

Keywords. Reverse Monte Carlo simulation; simple liquid; alkali metals; structure of liquid.

PACS Nos 61.20.Ja; 61.20.Ne; 02.70.-c

1. Introduction

Liquid metals differ from other classes of liquids such as molten salts primarily because of the presence of conduction electrons. Many elements show metallic behaviour in the liquid state, but their electronic band structures differ widely [1]. The structure factor of liquid metals is dominated by the repulsive core part of the effective interionic potential despite the fact that their pair potential are of a long-range oscillatory type [2]. The techniques of x-ray, neutron and electron diffractions have been employed to determine the (static) structure of non-crystalline materials using both transmission and reflection experiments. From the experimentally generated structural information, accurate peak positions and quantitative areas can be obtained; a three-dimensional model of the structure cannot be built solely on this intrinsically one-dimensional information [3].

The reverse Monte Carlo (RMC) simulation [4] provides a way of obtaining a three-dimensional picture of the disordered system from the intrinsically one-dimensional structural information. Howe *et al* [5] described elemental liquid structure modelled from experimental diffraction data using the RMC method. Liquid alkaline metals were investigated at particular temperatures, mainly at their melting points. Interesting results such as the pair distribution functions, $g(r)$, bond angle correlations $B(\cos\theta)$, and the average coordination number, n, were obtained from the RMC calculations. Nield *et al* [6] investigated the structural properties of caesium at its melting point and a few higher temperatures (30–1650°C).

The current calculations seek to give more detailed information on the structure of these metals not only at their melting points as discussed in [5], but also at temperatures higher than their melting points just as it was done for caesium [6]. This is done with a view of deducing information from such detailed calculations within a unified framework.

The lay-out of the current paper is as follows: in §2, we give some details of the reverse Monte Carlo (RMC) technique. We provide detailed information on the current calculation in §3. We discuss our results in §4 and end with conclusions in §5.

2. The reverse Monte Carlo (RMC) method

The structural behaviour regarding the positional correlation of particles has been studied extensively by two distinct techniques of computer simulations, such as the method of molecular dynamics (MD) and the metropolis Monte Carlo method usually called Monte Carlo (MC) method [7,8]. These methods are based on an interatomic potential and sometimes agree qualitatively with experiments depending on how well the chosen interatomic potential describes the reference liquid.

It is not clear and obvious in many cases how to alter the interatomic potential. This clearly limits the information that can be obtained from such modelling. The reverse Monte Carlo (RMC) simulation [4] has proved to be a powerful tool for modelling disordered structures [9,10]. The technique uses experimental data of the structure factor (most frequently diffraction data) as input and generates three-dimensional atomic configurations that are consistent with the experimental input data.

This goal is achieved by moving atoms around as in the MC method but instead of minimizing the energy, the squared differences between the experimental structure factor and the structure factor calculated from the computer configuration is minimized. This is considered as an important advantage considering the difficulty of obtaining energy (potential) for varying temperature, density (as used in the present work) and pressure. It also provides non-uniform information about the system, since all the data are fully utilized quantitatively rather than qualitatively.

The RMC technique provides a ground where many different sets or types of data can be combined simultaneously. It is general and can be easily adapted to different physical problems. The processes involved in RMC calculation are outlined below. Firstly, one starts with an initial configuration of atoms with periodic boundary conditions. This configuration is defined such that N atoms are placed in a box,

normally cubic, with periodic boundary conditions, by which one means that the box is surrounded by images of itself. For a cube of side L, the atomic number density ρ is given by

$$\rho = \frac{N}{L^3}. \tag{1}$$

This must be chosen to coincide with the required density of the system. Secondly, the radial distribution function for this old configuration is calculated using the equation

$$g_0^{\text{calc.}}(r) = \frac{n_0^{\text{calc.}}(r)}{4\pi r^2 \rho \Delta r}, \tag{2}$$

where $n_0^{\text{calc.}}$ is the number of atoms at a distance between r and $r + \Delta r$ from a central atom, averaged over all atoms as centres. The configuration size L should be sufficiently large that there are no correlations across the box, so that $g(r > \frac{L}{2}) = 1$. $g(r)$ is only calculated for $r < \frac{L}{2}$ and the nearest image convention is used to determine the atomic separation. Next is the transformation to the total structure factor using the Fourier transform:

$$S_0^{\text{calc.}}(q) = 1 + \frac{4\pi\rho}{q} \int_0^\infty r(g_0^{\text{calc.}}(r) - 1) \sin qr \, \mathrm{d}r, \tag{3}$$

where q is the wave vector. The next process involves the calculation of the difference between the experimental structure factor configuration $S^{\text{expt.}}(q)$ and calculated structure factor configuration $S_0^{\text{calc.}}(q)$;

$$\chi_0^2 = \sum_{i=1}^{n} [S_0^{\text{calc.}}(q_i) - S^{\text{expt.}}(q_i)]^2 / \sigma^2(q_i), \tag{4}$$

where the sum is over n experimental points and $\sigma(q_i)$ is a measure of experimental error.

The fifth process involves moving an atom at random. This is followed by computing the new radial distribution function $g_n^{\text{calc.}}(r)$ and structure factor $S_n^{\text{calc.}}(q)$ such that

$$\chi_n^2 = \sum_{i=1}^{n} [S_n^{\text{calc.}}(q_i) - S^{\text{expt.}}(q_i)]^2 / \sigma^2(q_i). \tag{5}$$

If $\chi_n^2 < \chi_0^2$, the move is accepted and the new configuration becomes the old. On the other hand if $\chi_n^2 > \chi_0^2$, the move is accepted with probability $\exp[-(\chi_n^2 - \chi_0^2)/2]$, otherwise it is rejected. Finally we repeat from step in eq. (5). These steps are repeated until χ^2 is sufficiently small and oscillates around an equilibrium value.

At this point, the configuration for which $S^{\text{calc.}}(q_i)$ agrees with $S^{\text{expt.}}(q_i)$ within the limits of experimental error can be evaluated. This algorithm is usually modified slightly by the imposition of some constraints. The most commonly used constraint is on the closest distance of approach of two atoms. Due to systematic

errors in the experimental data and limited data range, the data would not forbid some atoms from coming very close together. However, it is known that this is physically unrealistic and so an excluded volume is defined. While this is a very simple constraint on the structure, it is also very powerful since the imposition of both excluded volume and a fixed density restricts possible configurations that are consistent with the data.

3. RMC simulation and results

In this work, we have performed reverse Monte Carlo simulations for liquid alkali metals using 5000 atoms in each case. In all cases, the atoms are randomly placed in a cubic box but are allowed to move at a minimum distance apart, and the corresponding experimental structure factors $S(q)$ obtained from x-ray and neutron diffraction studies were used simultaneously as input data for Na at 100°C and 105°C, for K at 65°C and 70°C and for Cs at 30°C.

The x-ray diffraction data are taken from [2], while the neutron diffraction data are taken from [11]. Table 1 shows the densities used in the modelling for all the metals at different temperatures and was taken from [2].

The structure factor $S(q)$ was modelled using a modified version of an original code supplied by McGreevy *et al* [12] as described by the algorithm above. In all cases, the RMCA was run choosing a value of $\sigma = 0.01$ in order to get a good fit for the experimental data and also the values of the closest distance of approach were varied until a physically realizable $g(r)$ was obtained. We ensure that convergence was reached in all cases. In other words, the simulation was run until the value

Table 1. Densities used in the current calculations [2].

Metal	Temperature (°C)	ρ (g cm^{-3})	ρ (Å^{-3})
Na	100 and 105 double fit	0.928	0.02430
	200	0.903	0.02365
	300	0.881	0.02307
	550	0.823	0.02155
K	65 and 70 double fit	0.826	0.01270
	105	0.819	0.01259
	200	0.797	0.01225
	450	0.741	0.01139
Rb	40	1.476	0.01040
	100	1.448	0.01020
	200	1.397	0.00984
Cs	30 double fit	1.838	0.00830
	100	1.796	0.00810
	200	1.739	0.00785
Li	190	0.512	0.04400

of χ^2 remains fairly constant. The static structure factor $S(q)$, pair distribution function $g(r)$, coordination number, n, and the bond angle distribution $B(\cos\theta)$ were then determined from the final configuration.

4. Discussions

Analysis of these quantities gives more insight into the properties of the liquid alkali metals at temperatures indicated in the figures. Essentially, the RMC allows us to obtain more data from the diffraction data than what can be obtained purely from experimental results.

Figures 1 and 2 show the fits to the experimental diffraction data of $S(q)$ and the difference between the modelled $S(q)$ for molten Li, Na, K, Rb and Cs respectively at various investigated temperatures. In all cases, agreement between the RMC calculations and experimental values are excellent and this gives us confidence to use the configuration files to obtain more information about the liquid metals under investigation. The only cases for which there are notable differences between RMC results for $S(q)$ and diffraction data are for Na at 100 and 105°C, for K at 70°C and mostly for Cs at 30°C.

In those cases, we ascribe the differences to one or all of the following reasons:

1. The fits are to two sets of data based on two different diffraction techniques, viz. x-ray and neutron diffraction.
2. Apart from Cs, there is a little temperature difference, about ±5°C involved and this might have had some slight influence on the densities used.
3. For Cs, unlike in the other two liquid metals, we observed that the two sets of experimental data used were significantly different even in terms of the locations of the peaks and troughs. We assume this to be the major reason why there is more discrepancy for Cs even though the two experimental data are taken at the same temperature of 30°C.

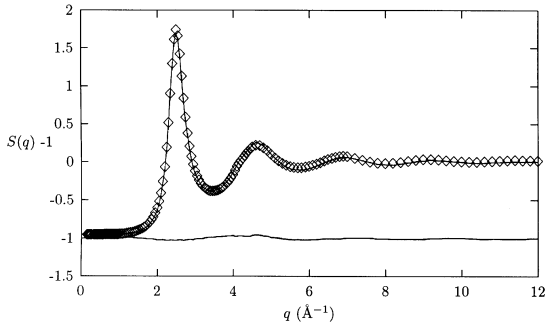

Figure 1. Static structure factor $S(q)$ for Li at the investigated temperature. Diamonds represent $S(q)$, from Waseda [2], solid lines passing through the experimental values are from the current simulation, while the solid lines close to -1 represent the difference between experimental and simulated values of $S(q) - 1$.

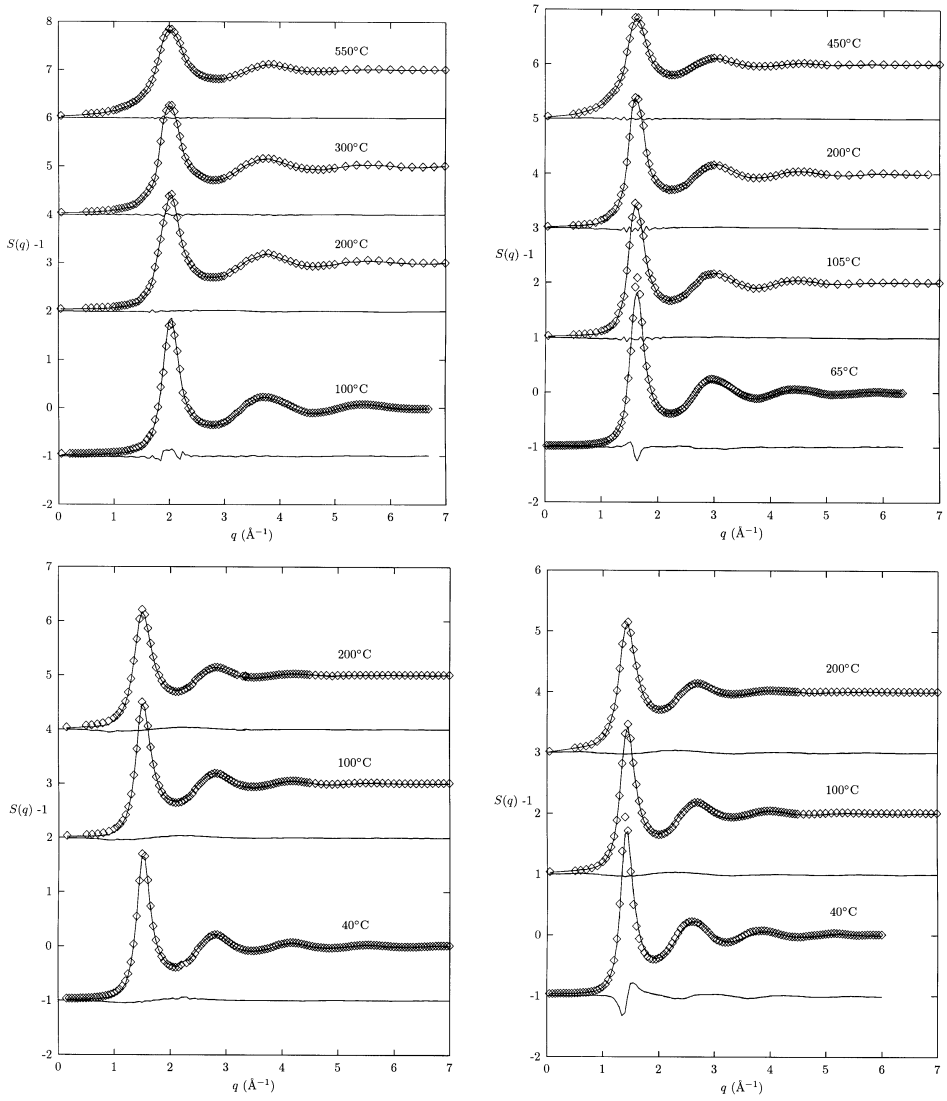

Figure 2. Static structure factor for Na, K, Cs and Rb at temperatures listed in the figures. Symbols and lines are as in figure 1. Upper graphs represent Na (on the left) and K while the lower graphs represent Cs (on the left) and Rb.

The pair distribution function $g(r)$ as derived from the RMC are shown in figures 3 and 4 for the set of cut-off distances finally adopted. The $g(r)$s obtained are all physically realizable except for Li and K at 105°C, 200°C and 450°C which show pre-peak. Cut-off distance did not give a better result by altering the values of the closest distance of approach. In fact, the values of the cut-off distance used here gave the best results. The pre-peaks are presumably indicative of slight errors

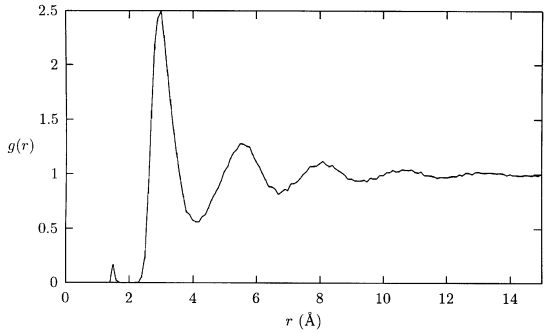

Figure 3. The $g(r)$ as obtained from RMC for liquid Li at 190°C.

in the experimental data. Nevertheless, we do not expect such errors to have any significant effect on our conclusions.

Table 2 gives the values of r_{p}, the position of the first peak, r_{c}, the cut-off distance, and r_{m}, the position of the first minimum of the pair distribution function $g(r)$. For Na, the values for r_{c}, r_{p} and r_{m} are fairly constant despite the significant variation in temperature.

The presence of a non-significant change in r_{p} suggests that the nature of the metallic bonding remains the same with increase in temperature. For K, r_{c} varies significantly with temperature but r_{p} is also relatively constant suggesting that the constant nature of the metallic bonding, r_{m}, slightly varies. Rb shows a decrease in r_{c} as temperature increases and fairly constant r_{p} and r_{m}. Cs shows the same trend as Rb except that r_{p} increases slightly with temperature.

Table 2. Table showing r_{c}, r_{p} and r_{m} of the pair distribution function, $g(r)$.

Metal	Temperature (°C)	r_{c} (Å)	r_{p} (Å)	r_{m} (Å)
Na	100 and 105 double fit	2.8	3.6	5.2
	200	2.9	3.7	5.1
	300	2.8	3.7	5.3
	550	2.8	3.6	5.3
K	65 and 70 double fit	3.6	4.6	6.5
	105	2.8	4.5	6.3
	200	2.8	4.6	6.5
	450	2.5	4.6	6.6
Rb	40	3.8	4.8	6.6
	100	3.6	5.0	6.7
	200	3.5	5.0	6.6
Cs	30 double fit	4.0	5.1	7.2
	100	3.8	5.2	7.2
	200	3.7	5.4	7.3
Li	190	1.8	2.9	4.0

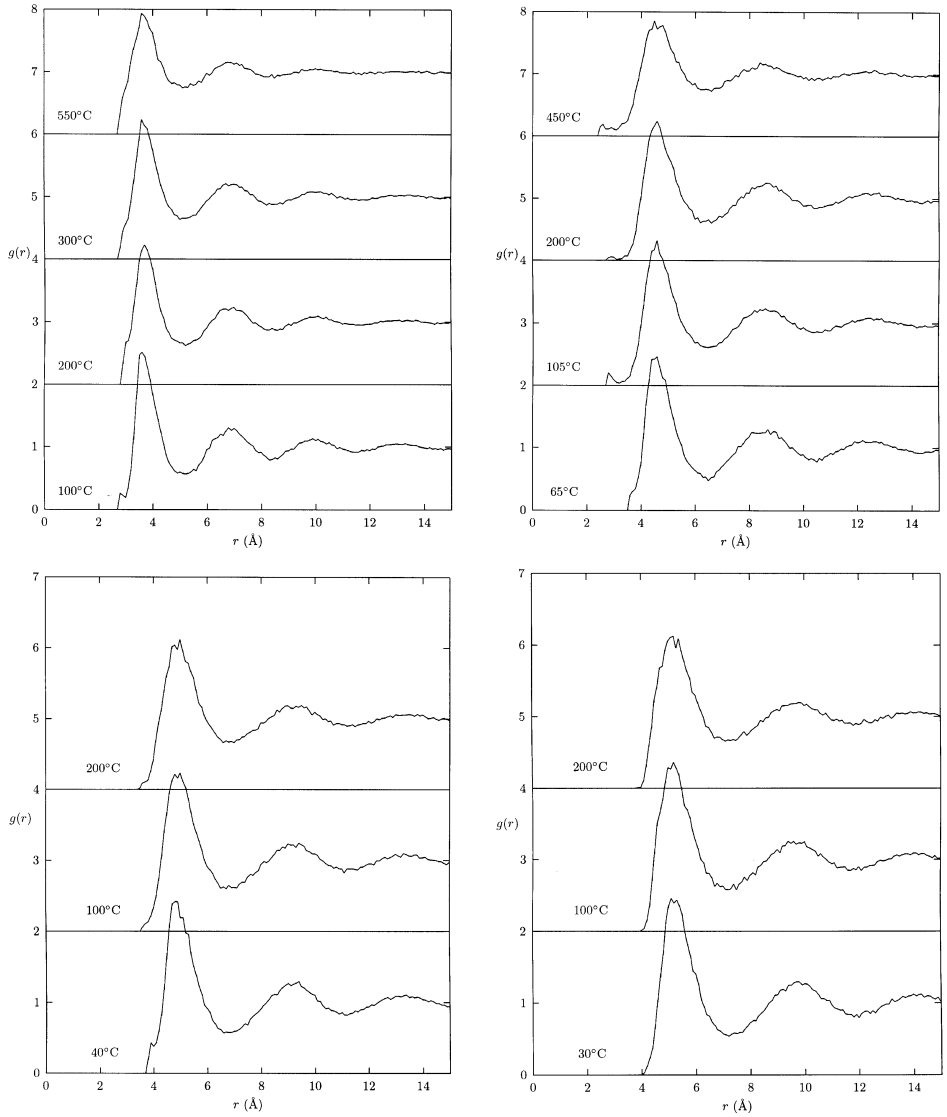

Figure 4. The $g(r)$ as obtained from RMC for liquid Na, K, Rb and Cs at indicated temperatures. The upper graphs represent Na (on the left) and K, while the lower graphs represent Rb (on the left) and Cs.

Li, even though looks simple, is a very complex liquid. It differs from other alkali metals because p states are absent from its core, and this implies that electron–ion interactions are quite strong. Furthermore, one could talk about state mixing effect which might arise from the proximity of s and p valence electron states [13]. It was considered only to see its characteristic structural properties when compared with other alkali metals. In general, as temperature increases, the height of the first peak

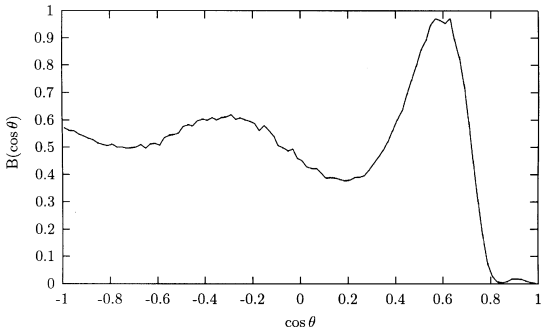

Figure 5. Distribution of the cosine of the bond angles, $B(\cos\theta)$ for liquid Li at 190°C.

in $g(r)$ decreases and the height of peaks after the first maximum also decreases in all the metals at their different temperatures.

Closer observation also shows that there are some unusual spikes at the first peaks of $g(r)$s for the highest temperature in all the metals. As discussed in [6], RMC modelling of expanded Cs, r_{p} and r_{m} of $g(r)$ are fairly constant, with $r_{\mathrm{p}} = 5.5$ Å and $r_{\mathrm{m}} = 7.5$ Å (The r_{m} at the highest temperature - 1650°C is 7.8 Å.) Simply, it means that the metallic bond has a mean length of 5.5 Å and a maximum length of 7.5 Å. Therefore Na, K, Rb, and Cs can be said to have their metallic bond lengths approximately within the range of 3.6–5.3 Å, 4.5–6.6 Å, 4.8–6.7 Å and 5.1–7.3 Å respectively.

Figures 5 and 6 show the distribution of the cosine of the bond angle, $B(\cos\theta)$, for Li, Na, K, Rb and Cs respectively. This is defined as the probability of two neighbours within r_{m} from a central atom forming an angle θ with the central atom. All the metals show the same variations and have two peaks. As temperature increases, the first peak flattens out, for example in Na at 550°C, it is almost structureless. This shows a distortion in the body-centred cubic (bcc) crystal structure of these metals at their melting points and temperatures above their melting points.

The distributions of the number of nearest neighbours of an atom at a distance less than a certain value from the reference atom for all the metals at various temperatures of interest were also considered. Here, the distance was taken to be the value corresponding to the value of the position of the first minimum, r_{m}.

The average coordination number, n, at those temperatures for all the metals was obtained from the calculated atomic configurations. Table 3 shows the temperature variation of the average coordination number for the molten metals as obtained from RMC. The average coordination numbers are large due to the supposed non-covalent bonding between them. There is a decrease in the average coordination number as the temperature increases.

This should be expected because as the temperature increases, the nearest neighbours of a central atom move further apart thereby causing a decrease in the average coordination number of the central atom.

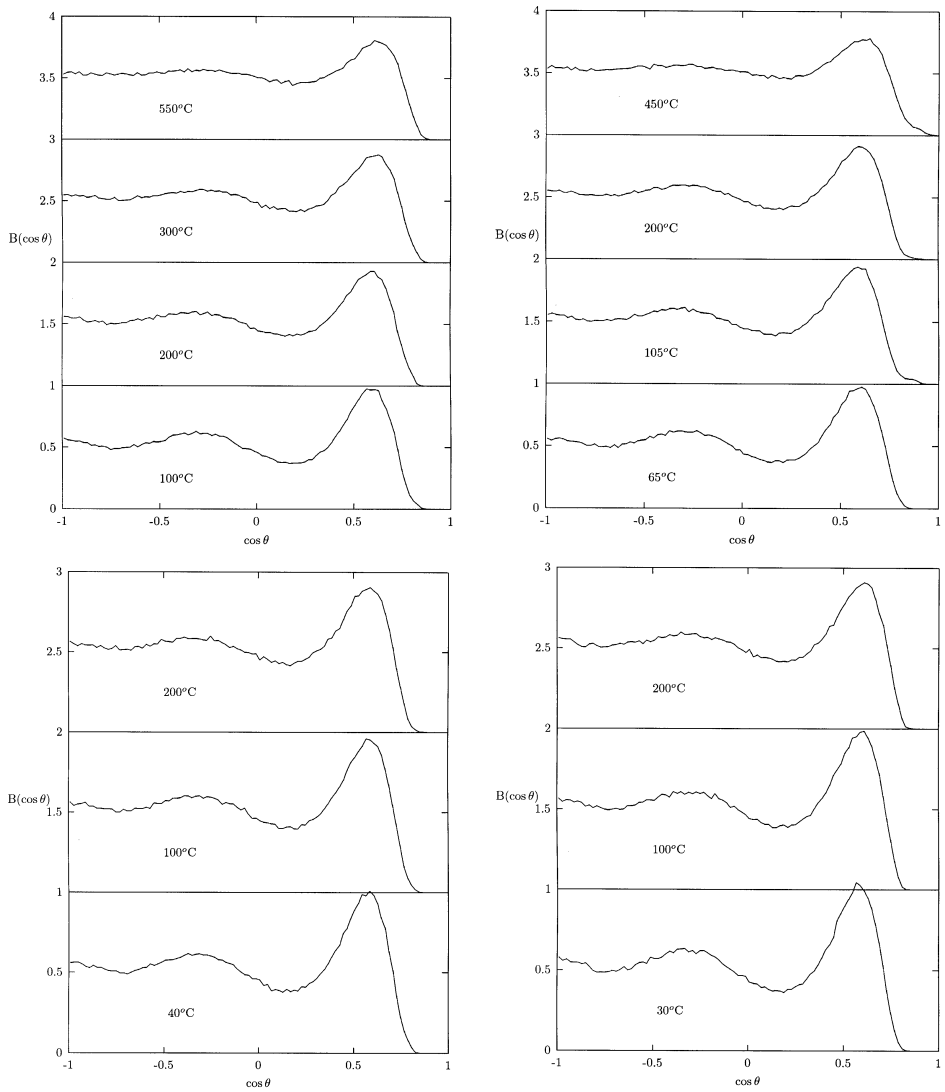

Figure 6. Distribution of the cosine of the bond angles for liquid Na, K, Rb and Cs at indicated temperatures. The upper graphs represent Na (on the left) and K while the lower graphs represent Rb (on the left) and Cs.

It was established for expanded caesium [6] that the average coordination number varies directly with density. However, the table also shows slight anomaly in the temperature–average coordination number variation at some temperatures. This probably is due to some errors in the experimental data used for the current calculations at those temperatures.

Our results show a general trend that the average number of nearest neighbours decreases when the density decreases and this is in agreement with those obtained from first principle MD and classical MD simulations [14,15].

Table 3. Table showing the temperature variation of the average coordination number for the liquid alkali metals as obtained from RMC.

Metal	Temperature (°C)	Average coordination number (n)
Na	100 and 105 double fit	13.6700
	200	12.8650
	300	13.5240
	550	12.6312
K	65 and 70 double fit	13.9068
	105	13.0812
	200	13.5076
	450	12.9240
Rb	40	12.6972
	100	12.7692
	200	11.9132
Cs	30 double fit	12.7628
	100	12.4040
	200	12.3368
Li	190	12.0672

5. Conclusion

A reverse Monte Carlo simulation of the static structure of liquid alkali metals – lithium (Li), sodium (Na), potassium (K), rubidium (Rb), and caesium (Cs) – at temperatures close to their melting points and higher temperatures has been successfully performed using 5000 atoms. The RMC calculations have shown that there is no significant change in their metallic bonding as temperature increases. Thus we conclude that the structure of liquid alkali metals is insensitive to the temperature within the investigated liquid regime.

The mean distance separating the nuclei of any two atoms bonded to each other was approximately estimated. In general, there is a distortion of the bcc crystal structure of these metals as temperature increases and their coordination numbers are high due to the presence of non-covalent bonding between them. It should be clearly stated here that the RMC method only provides information on the static structural properties of liquids, but not their dynamic properties thereby having limited applicability.

Nevertheless, if detailed information is to be obtained, quantitative agreement with the experimental data is very crucial.

Acknowledgement

We thank the Abdus Salam International Centre for Theoretical Physics, Trieste, Italy for financial support under Project PRJ-10.

References

[1] J P Hansen and I R McDonald, *Theory of simple liquids* (Academic Press, London, 1986)
[2] Y Waseda, *The structure of non-crystalline materials* (McGraw-Hill, New York, 1980)
[3] J K Walters and R J Newport, *Phys. Rev.* **B53**, 2405 (1988)
[4] R L McGreevy and L Pusztai, *Mol. Sim.* **1**, 359 (1988)
[5] M A Howe, R L McGreevy, L Pusztai and I Borzsak, *Phys. Chem. Liq.* **25**, 205 (1993)
[6] V M Nield, M A Howe and R L McGreevy, *J. Phys. Condens. Matter* **3**, 7519 (1991)
[7] I R McDonald, *Mol. Phys.* **23**, 253 (1972)
[8] R Car and M Parrinello, *Phys. Rev. Lett.* **55**, 2471 (1985)
[9] R L McGreevy, M A Howe, D A Keen and K N Clausen, *IOP Conference Series* **107**, 165 (1990)
[10] R L McGreevy, *J. Phys. Condens. Matter* **3**, 2471 (1991)
[11] W Van der Lugt and B P Alblas, *Handbook of thermodynamic and transport properties of alkali metals* edited by R W Ohse (Black-Well, Oxford, 1985)
[12] M A Howe, R L McGreevy and J D Wicks, RMCA Version 3: A general purpose reverse Monte Carlo code, October (1993) (unpublished)
[13] O Akinlade, S K Lai and M P Tosi, *Physica* **B167**, 61 (1990)
[14] M M G Alemany, J L Martins and B J Costa Cabral, *J. Non-Cryst. Solids* **347**, 100 (2004)
S R Bickham, O Pfaffenzeller, L A Collins, J D Kress and D Hohl, *Phys. Rev.* **B58**, R11813 (1998)
[15] S Munejiri, F Shimojo and K Hoshino, *J. Phys. Condens. Matter* **12**, 4313 (2000)